CNR-UNICA-USTO
Stay Report Document

Document Ref.: CUU-US-RD-001

Issue: 1

Prepared by: **Ahmed Nabil BELBACHIR**	Date: **23 July 2001**
Checked and Approved by: **Mohamed Faouzi BELBACHIR**	

Acknowledgment

The authors would like to thank the professor Alessandra Fanni for her help and warm reception at her institute. It is a great pleasure to work and collaborate with her. They want to thank her for all her great efforts to provide a wonderful working environment. The authors would like to thank all the team of the C ATS laboratory for their sympathy and help. Special thanks to Enrico Marongiu, Augusto Montisci, Barbara Cannas and Mario Lera.

The authors would also like to thank Bachisio Arca for his fruitful collaboration and all the team from CNR at Sassari.

Special thanks to the administration of the Electrical and electronic engineering institute for their help to make easy the accommodation rule. Thanks to Renata and Gina.

Contents

1. Acronyms and Abbreviations

BUSD	Biomass Ultra-Sonic Detector
CNR	Centro Nazionale di Ricerca
FFT	Fast Fourier Transform
HT	Hartley Transform
HW	HardWare
MSE	Mean Square Error
PCB	Printed Circuit Board
SW	SoftWare
TBD	To Be Defined
UNICA	UNIversità degli studi di CAgliari
USTO	University of Science and Technology of Oran

2. References

RD001 Automatic Optical Inspection of Electronic Devices Using Neural Networks (EANN01)

RD002 Alternative Neural Network Models for the Rain-Runoff Process (EANN01)

RD003 Neural Network Estimation of Crop Biomass by Ultrasonic Measurement (EANN01)

RD004 Project for the Realization of a System for a Quality Control of a Product in an Agro-alimentary Industry in Algeria

3. Introduction

Algeria and Sardinia are located in the same area around the Mediterranean sea. They share common problems related to the environment and the weather conditions. Therefore, the Institute of Electrical and Electronic Engineering at the University of Cagliari, the Institute for Monitoring of the Agro-ecosystems at Sassari and the Institute of Electronics at the University of Science and Technology of Oran decide to collaborate and unify their efforts to investigate on several projects related to these problems. The proposed projects are:

1- Printed circuit board inspection
2- Biomass measure of a vegetation using ultrasonic detector
3- Automatic and chemical analysis of the components of the essential oil extracted from the Mediterranean spot
4- Quality control of the products for an agro-alimentary industry
5- Improvement of the mathematical model for the estimation the evapo-transpiration of the vegetation
6- Design of a model for the estimation of the run-off from a water source to a dam
7- Design and implementation of a model to estimate and follow-up a pollution in an underground water reserve

In this contest, Prof. Mohamed Faouzi Belbachir and Dr. Ahmed Nabil Belbachir have visited the University of Cagliari. The aim of his stay was to study and evaluate the Algerian contribution on these projects. They have participated to 4 meetings and have got contact to several Italian researchers in order to define and agree on the participation form.

4. Meetings

4.1. Meeting 1. "University of Cagliari 10.07.2001 at 10h00"

Attendees: *A.N. Belbachir, B.Cannas, A. Fanni, M. Lera, E. Marongiu and A. Montisci*

A first meeting between Dr Belbachir and the Italian researchers has been performed. The main purpose was to get knowledge about the different available research topic and to investigate on the possibility to collaborate. The proposed research projects were as follows:

1. Biomass measure of a vegetation using ultrasonic detector
2. Printed circuit board inspection
3. Design of a model for the estimation of the run-off from a water source to a dam
4. Design and implementation of a model to estimate and follow-up a pollution in an underground water reserve

5. Automatic and chemical analysis of the components of the essential oil extracted from the Mediterranean spot
6. Quality control of the products for an agro-alimentary industry
7. Improvement of the mathematical model for the estimation the evapo-transpiration of the vegetation

4.2. Meeting 2. "University of Cagliari 13.07.2001 at 10h00"

Attendees: *A.N. Belbachir, M.F. Belbachir, B.Canna and A. Fanni*

A first contact between Prof Belbachir and the Italian researchers has been performed. The aim of this meeting was to introduce Prof. Belbachir to the different researchers and to get knowledge about the different activities performed at the institute of Electronic in Italy. A discussion about the different possibilities of cooperation and the work schedule have been made.

4.3. Meeting 3. "University of Cagliari 10.07.2001 at 15h00"

Attendees: *B. Arca, A.N. Belbachir, B.Cannas, A. Fanni, M. Lera, E. Marongiu and A. Montisci*

A meeting between the whole partners have been held at the university of Cagliari. Dr Arca from the University of Sassari have presented the different projects and given their status reports. The discussion about the projects was as follows:

1. Biomass measure of a vegetation using ultrasonic detector

The main problem related to this project was related to the detector device. The Biomass Ultra-Sonic Detector BUSD has been build in Florence in order to serve for the projects. It seems that the instrument is not reliable and the measurements for the same product are not repetitive. Furthermore, the real objective of this project is not completely clear. At the moment, the BUSD will be restored at Florence. It is also very important to clarify the main aim of the project.

2. Improvement of the mathematical model for the estimation the evapo-transpiration of the vegetation

The aim of this project is to develop an empirical model according to the existing mathematical model "Penman-Monteith" which can estimate the evapo-transpiration in a field using some implanted sensor inputs. The empirical model has the task to estimate more accurately the evapo-transpiration in this field. The accuracy level could be evaluated using a Lysimeter.

The input to the model are taken from several sensors of temperature, humidity, pressure, solar radiation, net radiation…etc.

An existing database is available for 80 years. Some models have already been developed using neural network and need to be improved.

3. Automatic and chemical analysis of the components of the essential oil extracted from the Mediterranean spot

The technical purpose is to describe the decomposition of the oil extracted from some plants using the NMR (Nuclear magnetic resonance). The set of elementary components constituting the oil should be enumerated. Dr. Arca has presented a poor data base which could define the real problem which could not be sufficient to develop a robust model or strategy. The objective of this research has to be clarified.

4. Quality control of the products for an agro-alimentary industry

The aim of this project is to control the quality of the products of an agro-alimentary industry using some techniques MRI (Magnetic Resonance Imaging)…etc. At the present time, there is no available database, and no experimental study about the reliability of the instrument has been made. The first objective is to collect a set of data in order to better locate the problem and to propose the expected solutions.

4.4. Meeting 4. "University of Cagliari 17.07.2001 at 14h30"

Attendees: *A.N. Belbachir, B.Cannas, A. Fanni, M. Lera, E. Marongiu and A. Montisci*

The aim of this meeting was to expose some problems related to the project PCB inspection and the rainfall-runoff process projects. A previous work has been already performed. It was intended to improve this work making use of deep study of the pre-processing steps. More description of these projects and their improvement could be found in the following sections.

5. Projects Description

5.1. Project 1. Printed Circuit Board (PCB) Inspection

5.1.1. Description

The purpose of this research topic is to build a robust program for the detection of defects in printed circuit boards for an industry. Indeed, a TBD inspection camera will be set at the end of an production line of printed circuit boards. It will be connected to a control PC. Their task is to inspect the defected board and to raise an alarm. The PC should be doted with a control program which could check an entire board in less than a minute and give a diagnostic report. The PCB will be loaded from a roll-band to the control box upon which will be fixed for minute.

Several boards are considered for the inspection. Therefore, the control program should be very flexible to cope with the different boards. Furthermore, several defects will be considered such as: absence of component on the PCB, displacement of component, poor solder join, component in a wrong place…etc.

For further details of the project see the document RD001

5.1.2. Experimental setup

A previous work has already been performed. A satisfactory results have been provided [1]. A software has been developed using the neural network. However, this program has been applied for a single board and has shown some imperfections whenever generalized to other boards. A deep study for this defect has been made.

A new image acquisition has been made as shown in Figure 1, using the following devices:

1- ***Digital camera:***

- ***A**uto-focus*
- Fast shutter speed
- Set at 17 meter far from the PCB

2- Two reflector lamps

- Power of 40 W each
- Luminous intensity of 540 cd
- Accent lighting (bleaching effect)
- Non faceted reflector (non-uniform distribution of the light)

3- PCB to inspect

- Contains 20 chips
- 3 defected solder joins

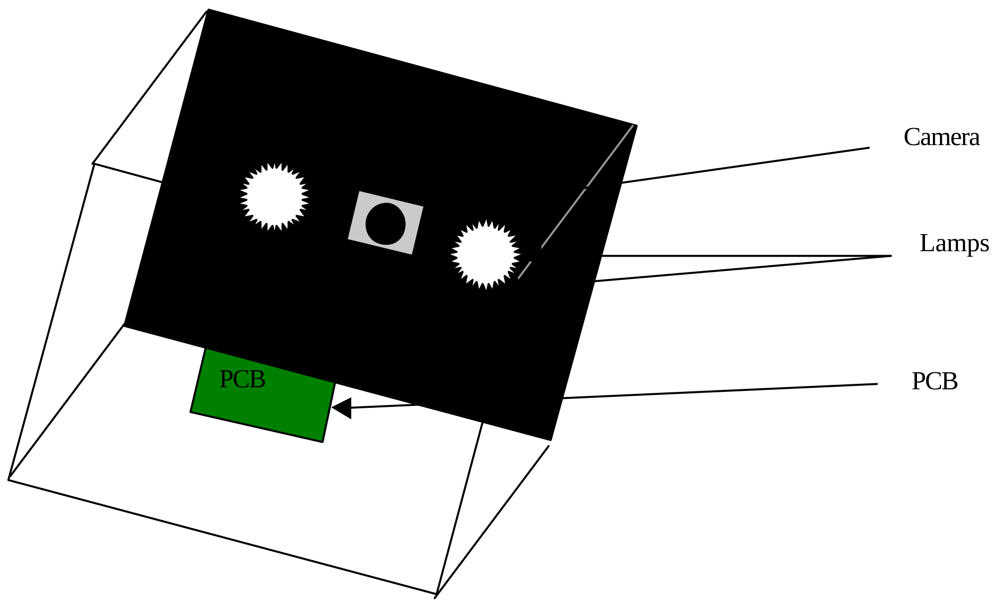

Figure 1. Representation of the PCB inspection setup (Image acquisition)

Four consecutive pictures have been taken for the same chip at the same setting with this setup in a dark room. However, two other pictures have been taken for the same chip with this setting in a lighted room with fluorescent lamps.

5.1.3. Work procedure

The concept of the PCB inspection procedure is depicted in Figure 2.

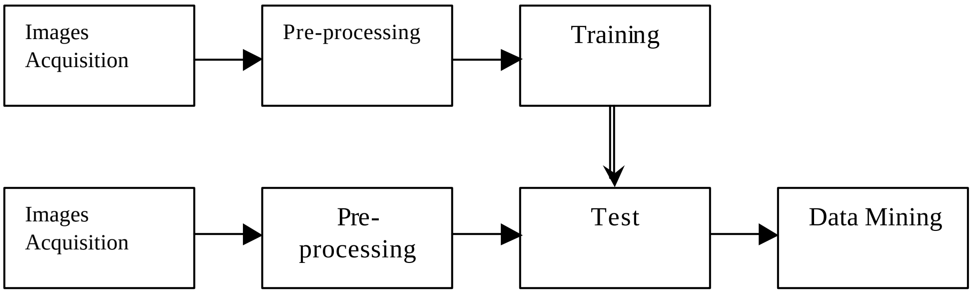

Figure 2. Concept of the PCB Inspection

A previous work has been already performed. Our aim is to cope with its imperfections whenever this concept is generalized. As we are using the neural network, it seems that the accuracy of the neural network depends mainly of the accuracy of their inputs. Therefore, we concentrate our work to study the images acquisition and the pre-processing steps to find out more accurate features for the neural network. We focus to study the following effects:

1- The effects of the lighting environment, the repeatability and accuracy of the camera on the acquired images

2- To study where the dominant information of the images is

3- The use of a more accurate feature extraction method which fits to our application

5.1.4. Experimental Study

5.1.4.1. Effect of the lighting environment and the camera accuracy

5.1.4.1.1. Introduction

To study these effects, we have performed the following experiments:

1- Take an image of a PCB 4 times in a dark room with only 2 reflector lamps (east and west of the board). As a results we have: image 1, image 2, image 3 and image 4.

2- Take two images to the same board with the same lighting with a lighted room with fluorescent lamps. As a results we have: image 5 and image 6.

3- Convert the images to the Grey scale where each pixel is represented in 8 bits (0-255)

4- We have performed the following comparisons:

- Image 1 and image 2
- Image 1 and image 5
- The average of images 1, 2, 3 and 4 with the image 1
- The average of images 1, 2, 3, 4, 5 and 6 with the image 1

5- From each image we only select the chip images, therefore we had decreased the number of pixels. For the same chip we had chip1_image1 chip1_image2, chip1_image3, chip1_image4, chip1_image5 and chip1_image6.

6- We have performed the following comparisons:

- Chip1_image 1 and chip1_image 2
- Chip1_image 1 and chip1_image 5
- The average of chip1_images 1, 2, 3 and 4 with the chip1_image 1
- The average of chip1_images 1, 2, 3, 4, 5 and 6 with the chip1_image 1

5.1.4.1.2. Results

The following figures are the results of the comparison for the whole images with a resolution of 480x290. The comparison is only performed for the first 100 pixels. The comparison for the other pixels behave more or less in the same shapes.

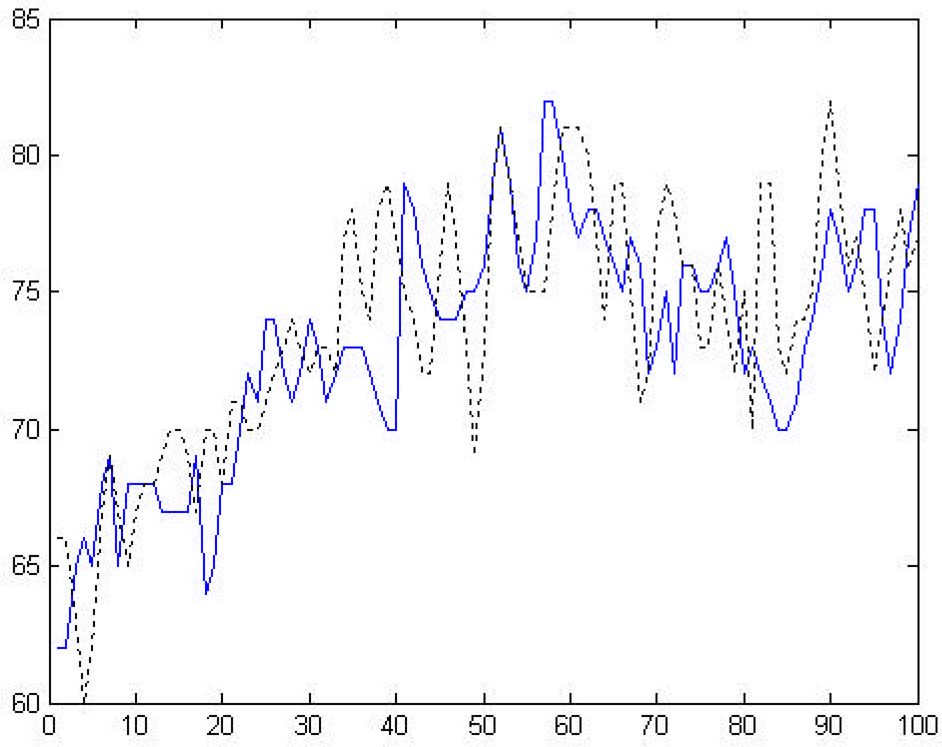

Figure 3. Comparison between image1 (solid line) and image2 (dashed line). Mean difference=3.01 mean(image1)=81.8, mean(image2) = 82.3

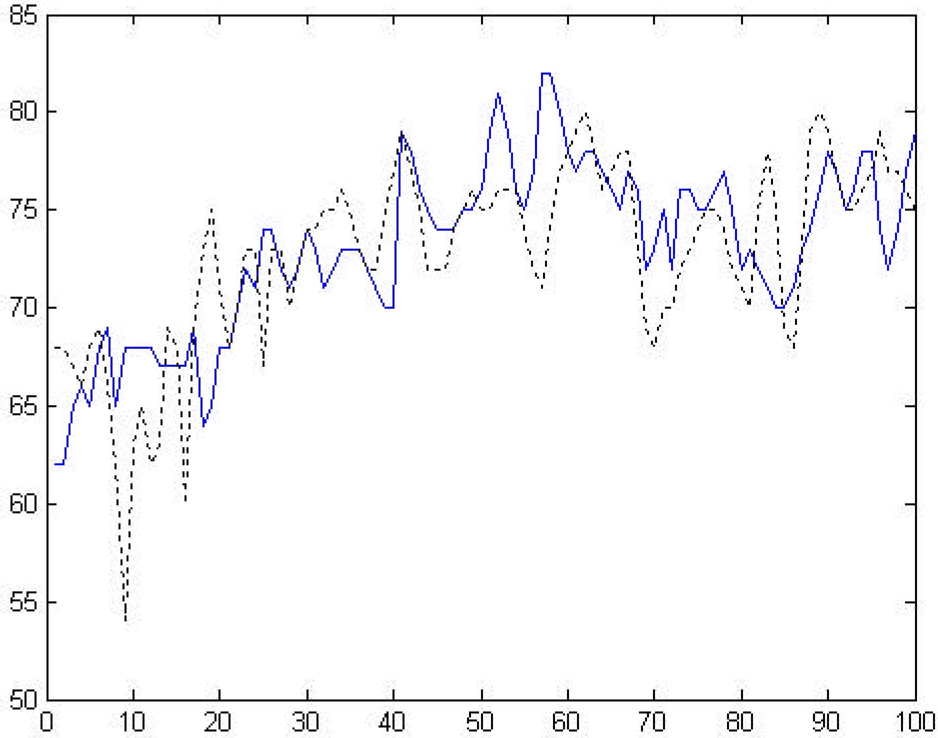

Figure 4. Comparison between image1 (solid line) and image5 (dashed line). Mean difference=6.03 mean(image1)=81.8, mean(image2) = 83.7

From Figure 3 and Figure 4, it could be noticed that the pixel representation for the same board taken on different time are quite different. This could be explained by the non uniform distribution of the light and the poor accuracy of the camera. It could also be noticed that the standard deviation between two images with a bright room (fluorescent lamps) at Figure 4 is much bigger than that taken in a dark room (Figure 3). We conclude that an acquired image is not repeatable. In the following experiments we integrate over the time in order to decrease the environment effects.

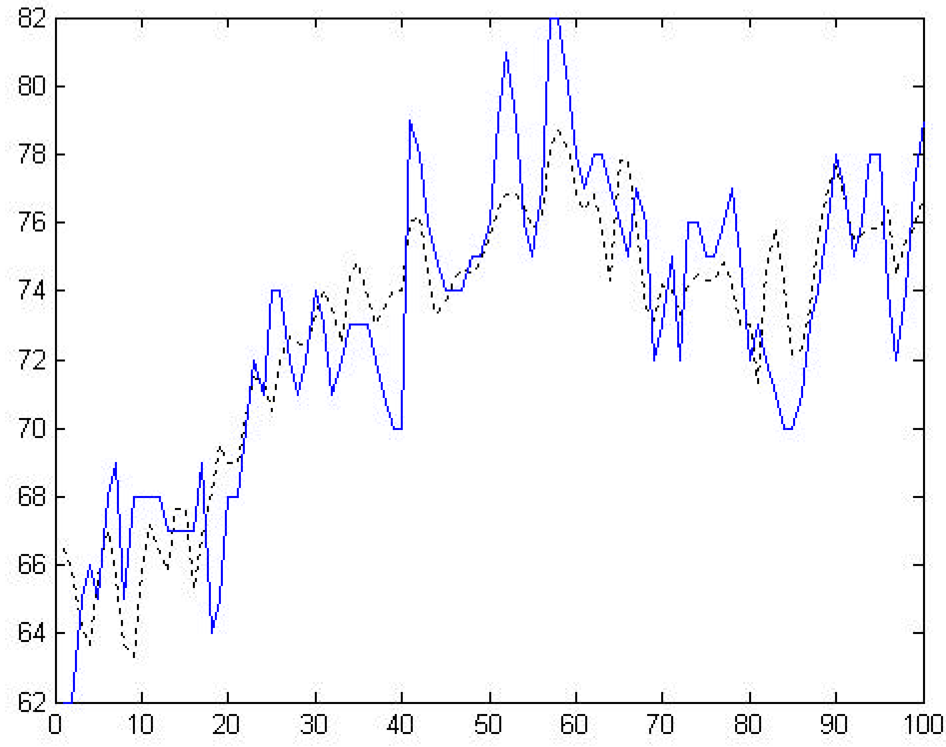

Figure 5. Comparison between image1 (solid line) and the average of the images 1,2,3 and 4 (dashed line). Mean difference=1.92 mean(image1)=81.8, mean(image2) = 81.5

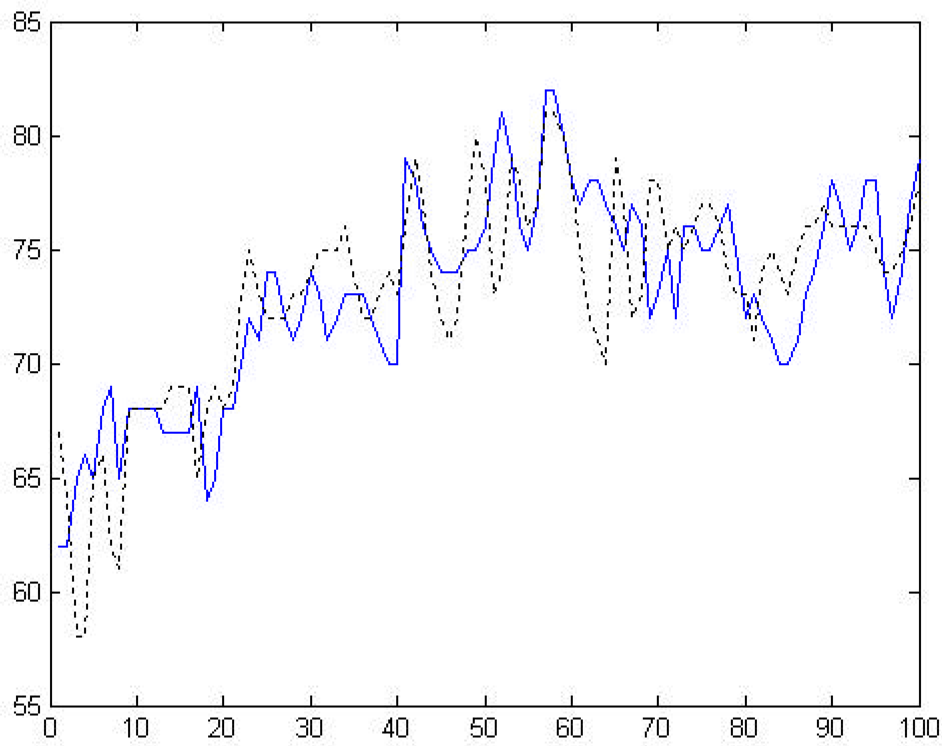

Figure 6. Comparison between image1 (solid line) and the average of the images 1,2,3,4,5 and 6 (dashed line). Mean difference=2.63 mean(image1)=81.8, mean(image2) = 82.4

From these experiments, we notice that the integration over the time has increased the accuracy of the acquisition. This is represented by the decrease of the mean error between the integrated images and the actual images. The integration has more effects for the same lighting device (Figure 5) than different lighting (Figure 6).

The same comparison have been performed for a reduced images of 180x140 pixels which only contains the same chip taken at different time ticks. The comparison is only performed for the first 100 pixels

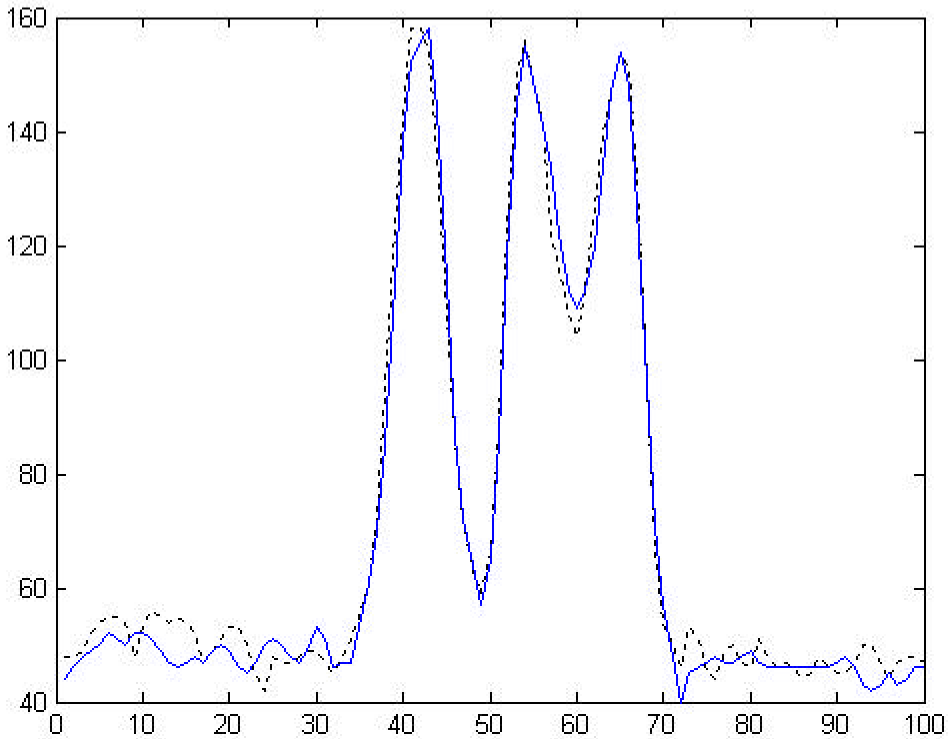

Figure 7. Comparison between chip1_ image1 (solid line) and chip1_ image2 (dashed line). Mean difference=3.43 mean(image1)=52.6, mean(image2) = 54.2

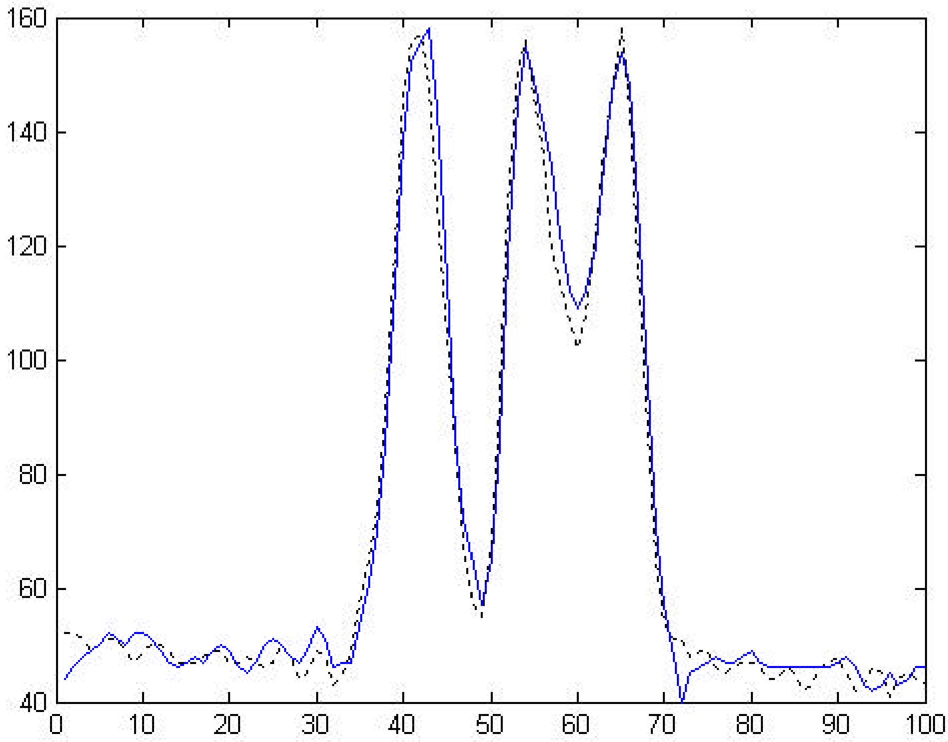

Figure 8. Comparison between chip1_image1 (solid line) and chip1_image5 (dashed line). Mean difference=3.8 mean(image1)=52.6, mean(image2) = 52.7

From Figure 7 and Figure 8, it could be noticed that the image segmentation give more accurate pixel representation for the same board taken on different time. Furthermore, the two figures have more or less the same shape for a bright region. However, the mean distribution of the error is always high due to non uniform light distribution and the non repeatability of the camera. In the following experiments we integrate over the time in order to decrease the environment effects.

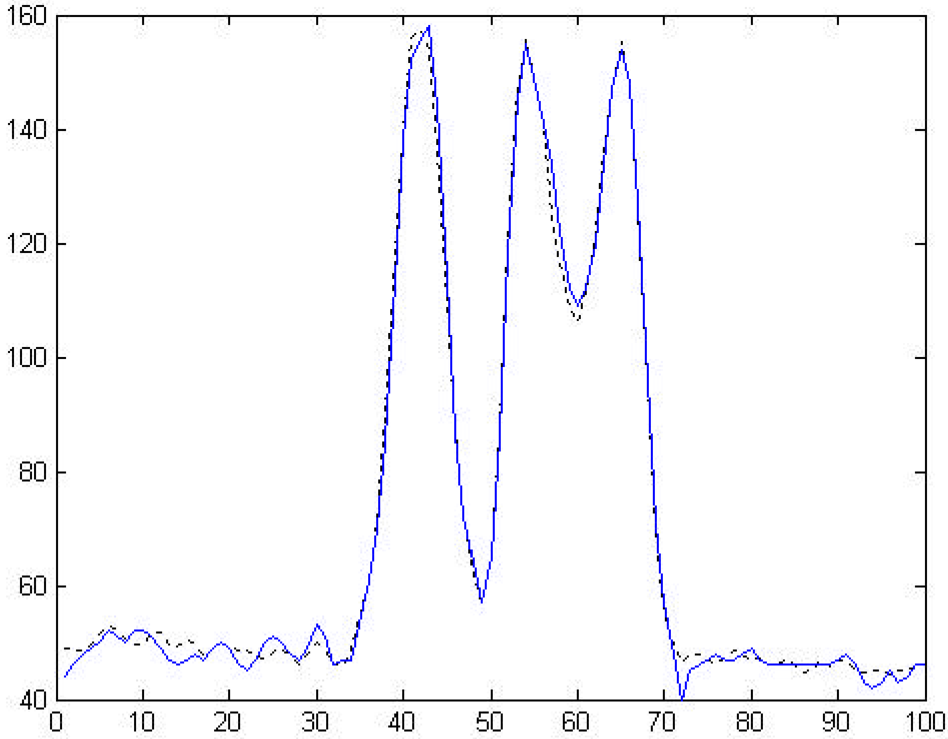

Figure 9. Comparison between chip1_image1 (solid line) and chip1_images 1,2,3 and 4 (dashed line). Mean difference=2 mean(image1)=52.6, mean(image2) = 53.3

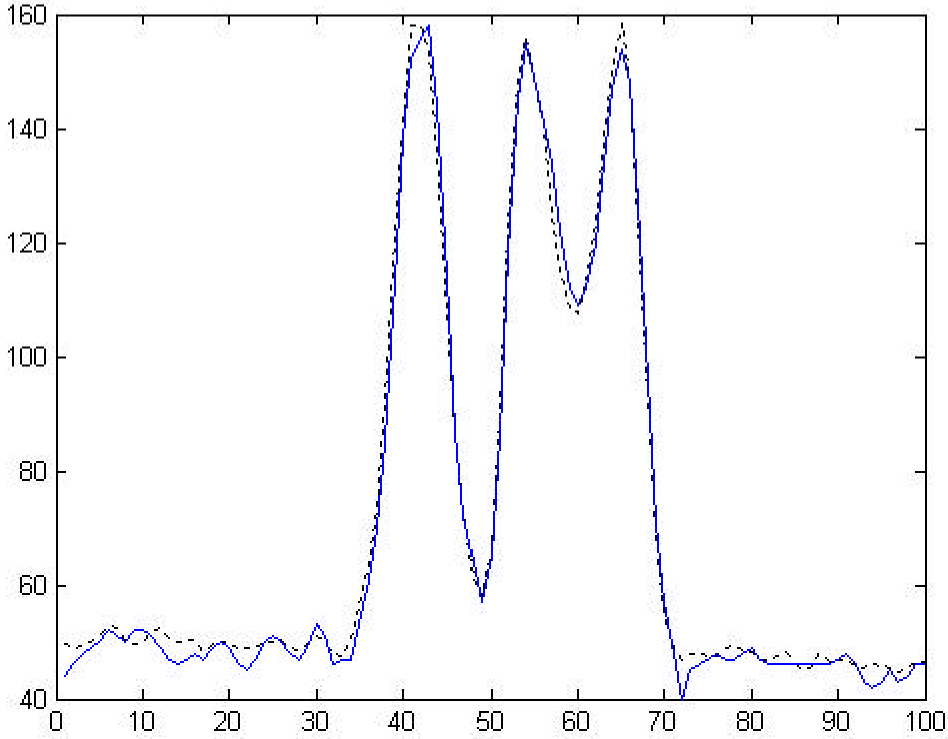

Figure 10. Comparison between chip1_image1 (solid line) and chip1_images 1,2,3,4,5 and 6 (dashed line). Mean difference=2.9 mean(image1)=52.6, mean(image2) = 54.1

From these experiments, we notice that the integration over the time has increased the accuracy of the acquisition. This is represented by the decrease of the mean error between the integrated images and the actual images. The integration has more effects for the same lighting device (Figure 9) than different lighting (Figure 10). Comparing these images (180x140) to the other images (480x290), we notice that the noise due to the acquisition environment has decreased.

5.1.4.1.3. Conclusions and Recommendations

From these experiments, it has been concluded that the accuracy of the image acquisition depends on its repeatability. The acquisition noise is related to several factors:

1. The non uniform distribution of the light
2. The non temporal fidelity of the light
3. The repeatability and accuracy of the camera

To decrease the impact of these factor, we propose the following solution

1. The use of the aluminum reflector Halogen lamps which present the following advantages:
   - An uniform distribution of the light
   - Up to 80% reduction in bleaching effect
   - For a 50 Watt lamp the luminous intensity is 12500 cd
2. The equi-distribution of the lamps around the PCB. 4 lamps (North-West-South-East) are recommended
3. More accurate acquisition camera (high repeatability)

5.1.4.2. Study of the effect of the acquisition noise on the FFT of the images

5.1.4.2.1.Introduction

To study these effects, we have performed the following experiments:

1- Use the FFT of the images of the same chip with the resolution 180x140.

2- We have calculated the magnitude and phase of the images

3- We have performed the following comparisons:

- Magnitude and phase of the chip1_image 1 and chip1_image 2
- Magnitude and phase chip1_image 1 and chip1_image 5
- Magnitude and phase of the average of chip1_images 1, 2, 3 and 4 with the chip1_image 1
- Magnitude and phase of the average of chip1_images 1, 2, 3, 4, 5 and 6 with the chip1_image 1

5.1.4.2.2. Results

Table 1 and Table 2 contain the results of the comparison respectively of the magnitude and the phase of the FFT for the different images of the same chip. The image resolution is 180x140 pixels.

	Mean Difference	Mean of A	Mean of B
A=chip1_image1 and B=chip1_image2	320	1500	1663
A=chip1_image1 and B=chip1_image5	437	1500	1600
A=chip1_image1 and B = average chip1_image1,2,3 and 4	210	1500	1580
A=chip1_image1 and B = average chip1_image1,2,3,4,5 and 6	251	1500	1620

Table 1. Comparison between the FFT magnitude of the different images

	Mean Difference	Mean of A	Mean of B
A=chip1_image1 and B=chip1_image2	$-1.2\ 10^{-17}$	$1.25\ 10^{-4}$	$1.25\ 10^{-4}$
A=chip1_image1 and B=chip1_image5	$7.4\ 10^{-18}$	$1.25\ 10^{-4}$	$1.25\ 10^{-4}$
A=chip1_image1 and B = average chip1_image1,2,3 and 4	$5\ 10^{-18}$	$1.25\ 10^{-4}$	$1.25\ 10^{-4}$
A=chip1_image1 and B = average chip1_image1,2,3,4,5 and 6	$7\ 10^{-18}$	$1.25\ 10^{-4}$	$1.25\ 10^{-4}$

Table 2. Comparison between the FFT phase of the different images

From these tables, we notice that the integration over the time has increased the accuracy of the acquisition (see the magnitude and the phase). This is represented by the decrease of the mean error between the integrated images and the actual images. The integration has more effects for the same lighting device (row 4) than different lighting (row 5). Comparing the two tables, we can notice that the phase is less sensitive to the acquisition noise (lighting) than the magnitude. This is represented by the small difference between two images taken at different times step as shown in Table 2 ($5\ 10^{-18}/1.25\ 10^{-4}$). However, for the amplitude the noise acquisition has more impact as shown in Table 1 (210/1500).

5.1.4.2.3.Conclusions and recommendations

The FFT seems to provide accurate input for the preprocessing step whenever the spectral phase is used. It seems less sensitive to the acquisition environment.

5.1.4.3.Study of the position of the relevant information in the images

5.1.4.3.1Introduction

To study the position of the relevant information on the FFT decomposition of the images, the following experiments have been performed:

1- Take the image of one chip 6 times (4 times in the dark room and 2 times in a lighted room): chip1_image1 chip1_image2, chip1_image3, chip1_image4, chip1_image5 and chip1_image6.

2- Perform the FFT and extract the amplitude and the phase

3- Using the Paint Shop Pro program, we include a defected pin to the six images: def1_image1 def1_image2, def1_image3, def1_image4, def1_image5 and def1_image6.

4- Perform the FFT and extract the amplitude and the phase

5- We have performed the following comparisons on the magnitude and phase of the images:

- Chip1_image 1 and def1_image 1
- Chip1_image 1 and def1_image 5
- The average of chip1_images 1, 2, 3 and 4 with the def1_image 1
- The average of chip1_images 1, 2, 3 and 4 with the def1_images 1, 2, 3 and 4

5.1.4.3.2.Results

The aim of this experiment is to show where the relevant information of the image is by the detecting the position of the relevant variation between the defected and safe boards.

1. Comparison of the magnitude

The first comparison has been performed between the FFT magnitudes of the images with the good solder join and those with the bad solder join. For a better view of the resulted 3D images a superposition between the x and y axes has been performed. The y-axis which contains the 180 pixels is on the right of the figure, where the x-axis which contains the 140 pixels is on the left of the figure. The z-axis represents the absolute error between the images of the same chip with and without a defected solder join.

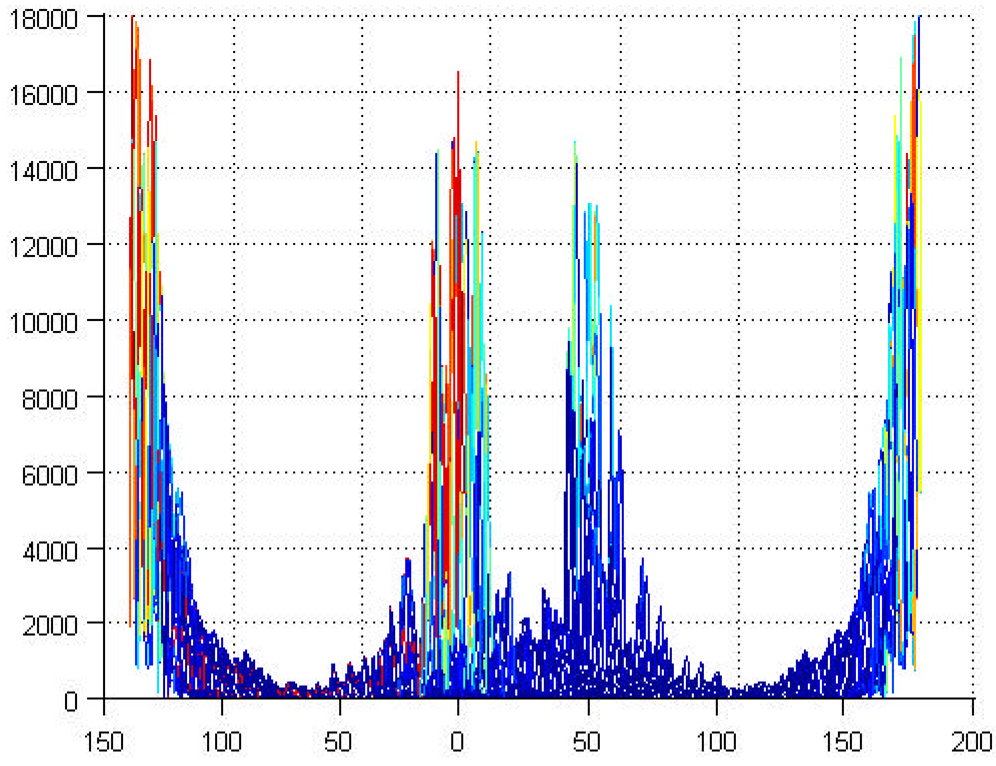

Figure 11. Comparison of the magnitudes between chip1_image 1 and def1_image 1 (maximum error = 17931 at pixel(140,2) and pixel(2,180), second maximum error = 17790 at pixel(138,2) and pixel(4,180))

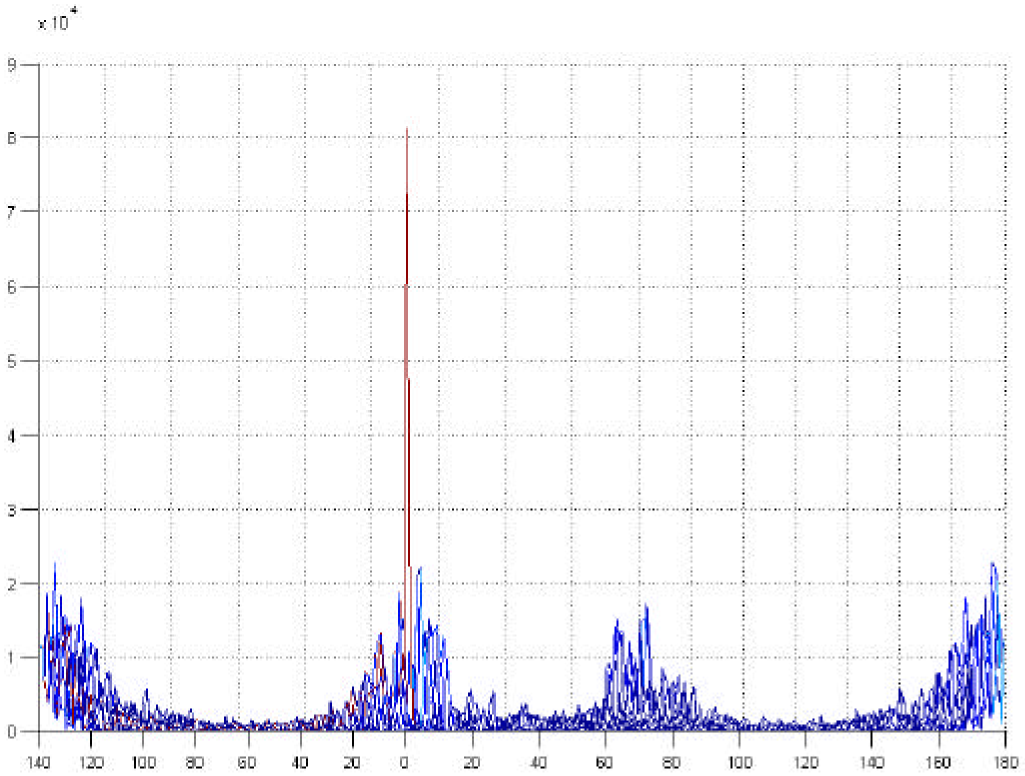

Figure 12. Comparison of the magnitudes between chip1_image 1 and def1_image5 (maximum error = 81121 at pixel(1,1), second maximum error = 22804 at pixel(2,177))

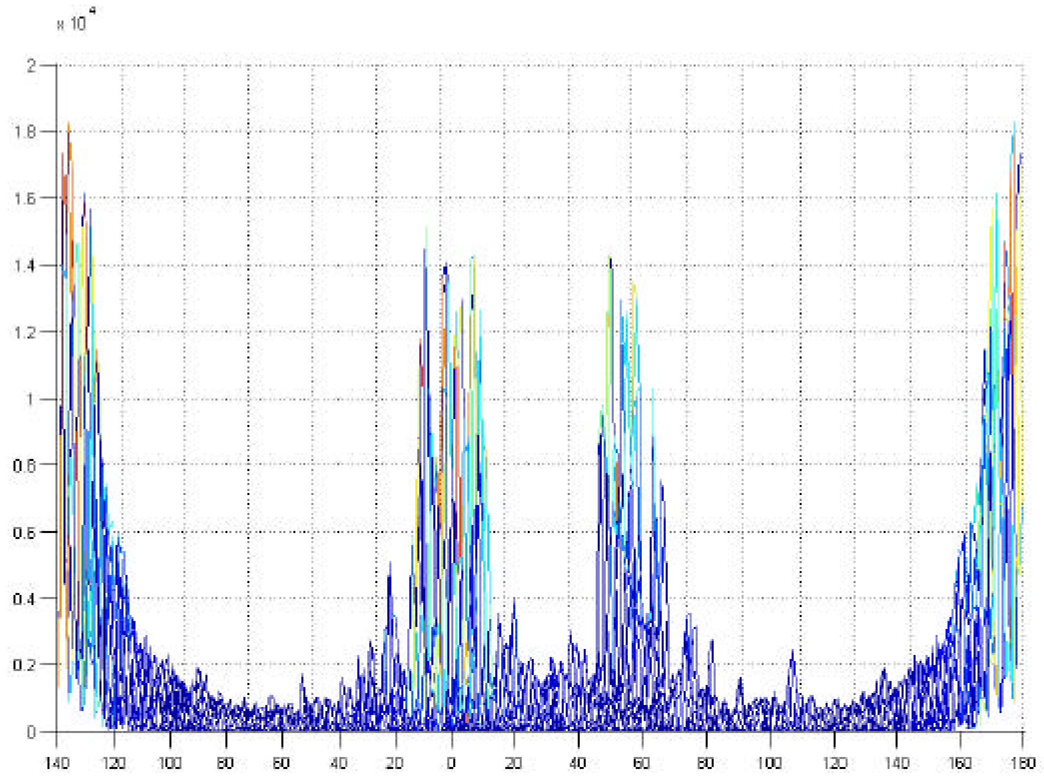

Figure 13. Comparison of the magnitudes between the average of chip1_images 1,2,3 and 4 and def1_image 1 (maximum error = 18244 at pixel(4,180) and pixel(138,2), second maximum error = 17319 at pixel(2,180) and pixel(140,2))

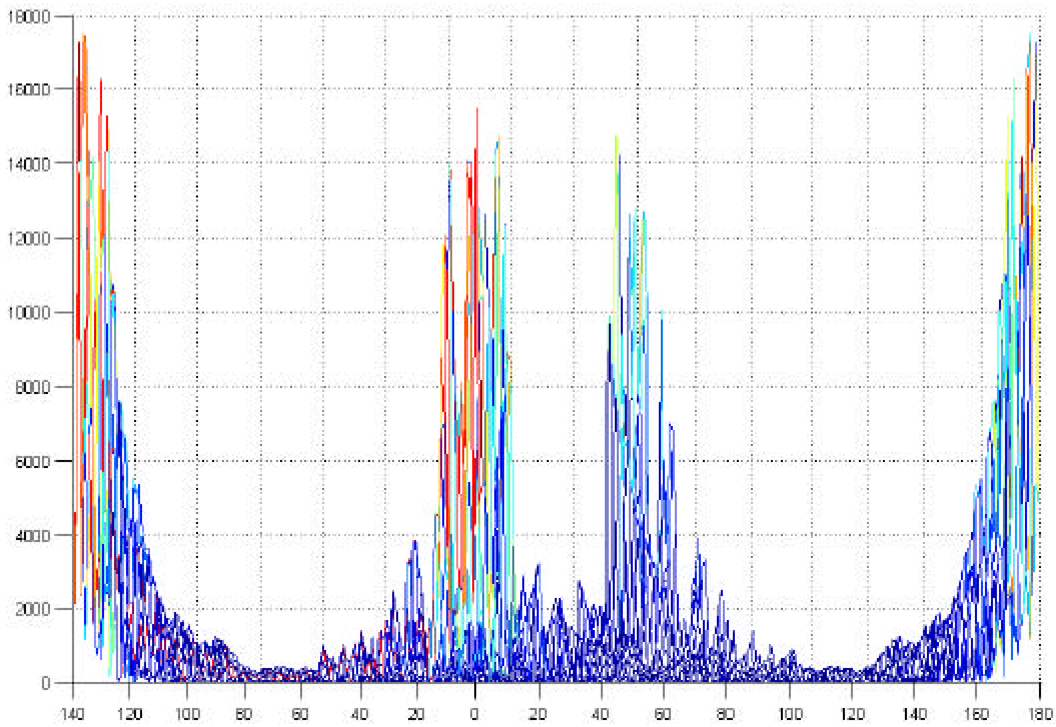

Figure 14. Comparison of the magnitudes between the average of chip1_images 1,2,3 and 4 and the average of def1_images 1,2,3 and 4 (maximum error = 17481 *at pixel(4,180)* and pixel(138,2), *second maximum error =* 17265 *at pixel(2,1*80*)* and pixel(140,2)*)*

From Figure 11, Figure 12, Figure 13 and Figure 14 we notice the following remarks:

- The relevant information is located on four regions, on the four corners of the magnitude matrices
- A double symmetry could be noticed
- The maximum errors are located on the two regions (first columns, last rows) and (last columns, first rows)
- On Figure 11, where the comparison between two images (good and bad solder join) of the same chip taken at the same instant t, we notice that the main differences are located on the two coins (first columns, last rows) and (last columns, first rows)
- On Figure 12, where the comparison between two images (good and bad solder join) of the same chip taken at different instant t with different lighting conditions, we notice that the main difference is located in the first sample (continuous component). This sample represent the background of the image. We can notice that the amplitude is very sensitive to the image acquisition conditions. Skipping this sample, the main differences are always located on the two coins (first columns, last rows) and (last columns, first rows)
- On Figure 13, where the comparison between two images (one image with good solder join and integrated four images with bad solder join taken at different instant) of the same chip, we notice that

the main differences are located on the two coins (first columns, last rows) and (last columns, first rows). This differences have increased compared to Figure 11.

- On Figure 14, where the comparison between two images (integrated four images with good solder join and integrated four images with bad solder join taken at different instant) of the same chip, we notice that the main differences are located on the two coins (first columns, last rows) and (last columns, first rows). This differences have decreased compared to Figure 11.

2. Comparison of the phase

The same comparison performed with the magnitude will be applied with the spectral phase of the FFT of the images. For a better view of the resulted 3D images a superposition between the x and y axes has been performed. Taking into account the anti-symmetry of the spectral phase, we only draw on the y-axis which contains the 91 pixels which is on the right of the figure, however the x-axis which contains the 140 pixels is on the left of the figure. The z-axis represents the absolute error between the images phases of the same chip with and without a defected solder join.

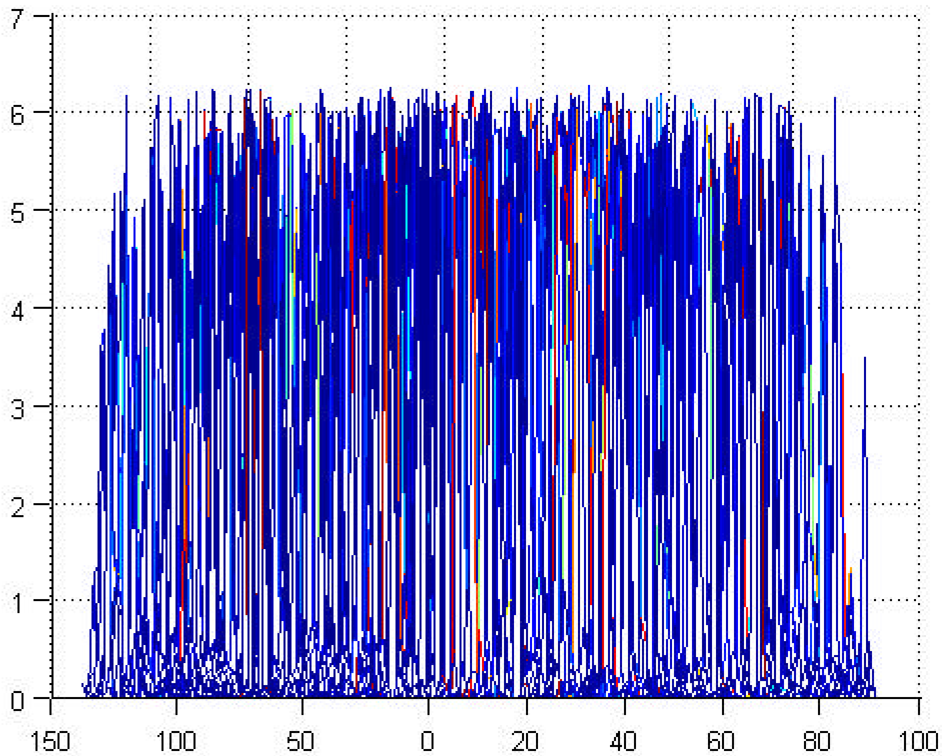

Figure 15. Comparison of the phases between chip1_image 1 and def1_image 1 (maximum error = 6.2641 at pixel(107,87), second maximum error = 6.2484 at pixel(31,52))

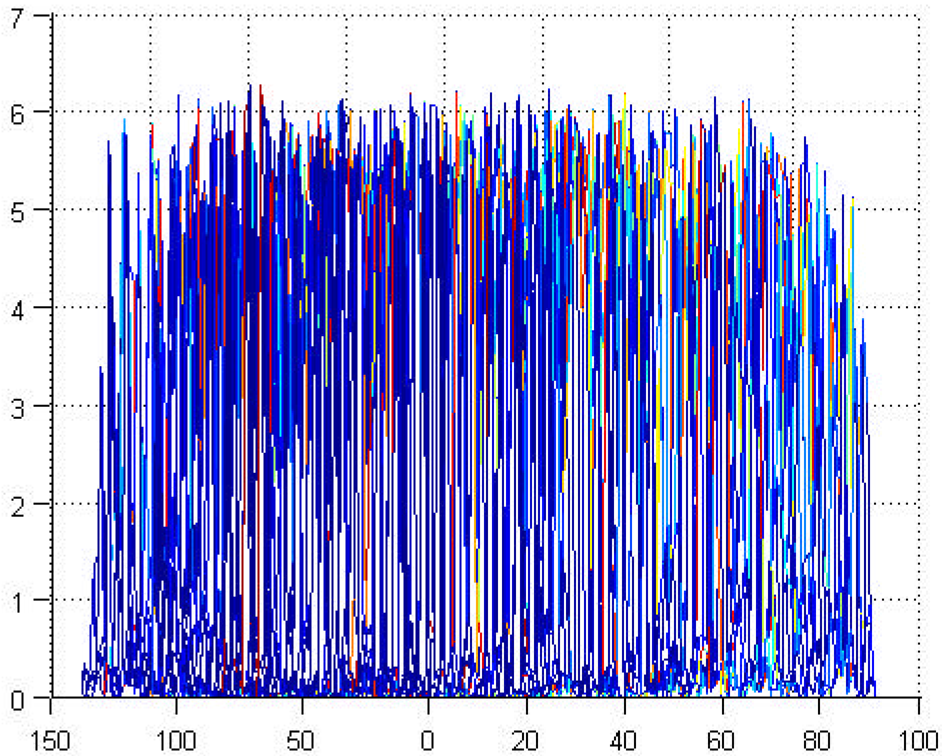

Figure 16. Comparison of the phases between chip1_image 1 and def1_image 5 (maximum error = 6.2558 at pixel(69,1) and pixel(73,1), second maximum error = 6.2114 at pixel(15,32))

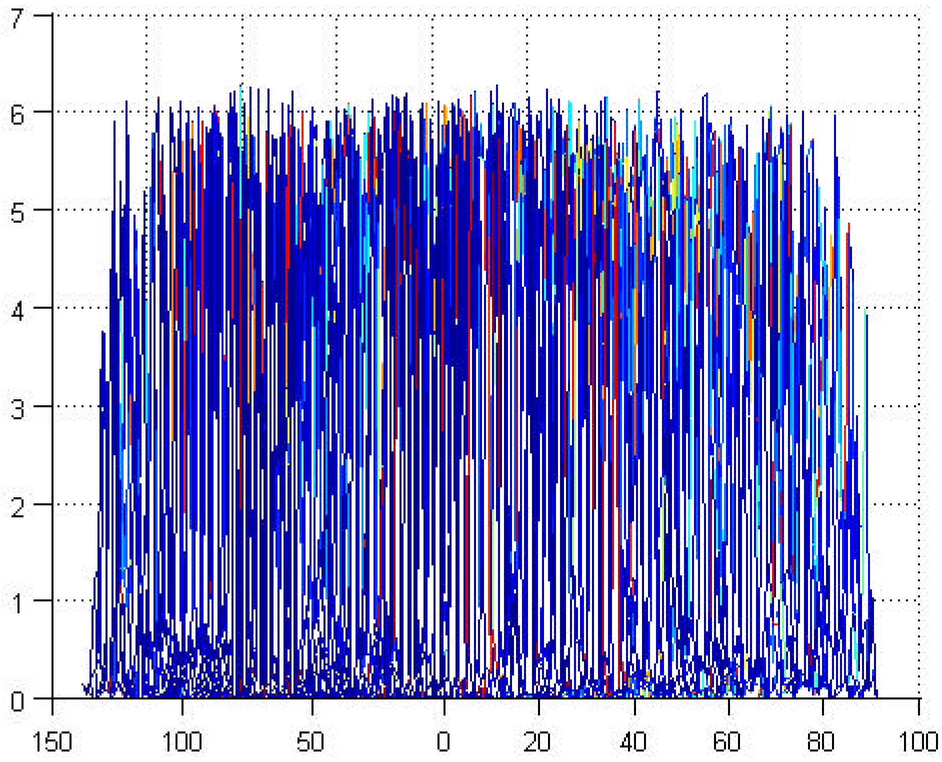

Figure 17. Comparison of the phases between the average of chip1_images 1,2,3 and 4 and def1_image 1 (maximum error = 6.2618 at pixel(13,18), second maximum error = 6.2546 at pixel(105,15))

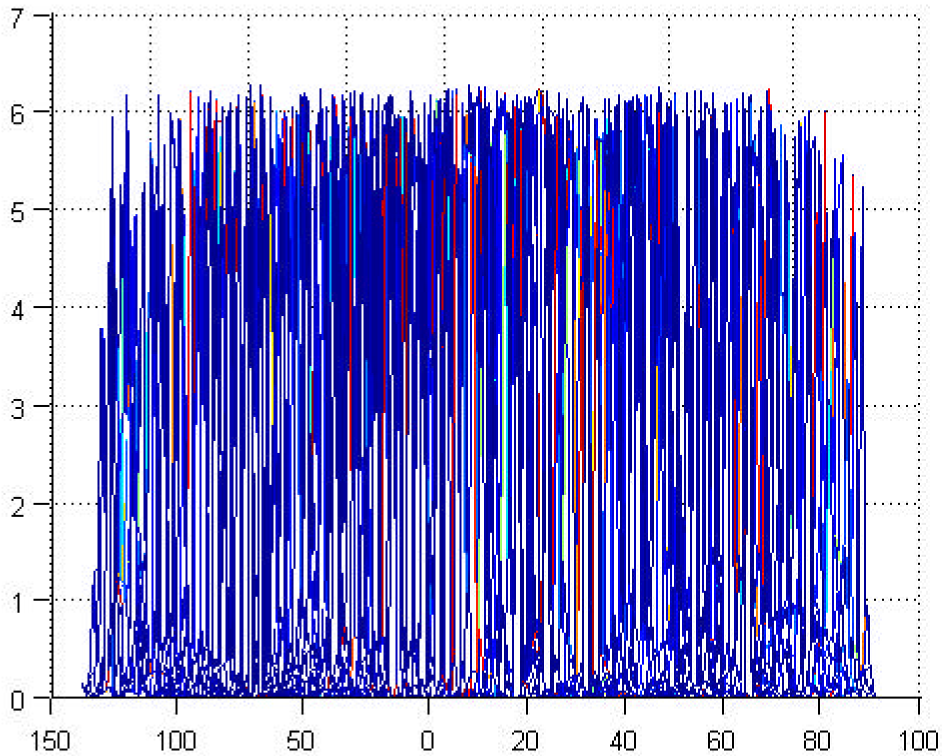

*Figure 18. Comparison of the phases between the average of chip1_images1,2,3 and 4 and the average of def1_images1,2,3 and 4 (maximum error=*6.264 *at pixel(69,1)* and pixel(73,1), *second maximum error=6.2502 at pixel(129,74))*

From Figure 15, Figure 16, Figure 17 and Figure 18 we notice the following remarks:

- It is quite difficult to locate the relevant information on the spectral phase distribution
- The maximum error (about 2π) is located on several regions depending on the images
- The temporal information (the acquisition noise due to the lighting conditions) seems to not affect the spectral phase.
- It is very difficult to evaluate the effect of the integration over the time of the four images. To evaluate this parameter, see the application of this method on the following sections

5.1.4.3.3.Conclusions and recommendations

The use of a FFT seems consistent to distinguish between two PCBs with different defects. This is depicted by the representative error between two boards using the frequential distribution (Magnitude and phase). However, the magnitude seems more sensitive to the acquisition noise (lighting conditions) than the phase.

We recommend to use the spectral phase information as an input parameters to the neural network. However, the magnitude information seems representative whenever an integration over time is required.

5.1.4.4. The use of a more accurate feature extraction method which fits to our application

5.1.4.4.1.Introduction

Th aim of this phase was to implement a good preprocessing algorithm by combining the phase and magnitude information of the FFT. Indeed, we find out to use the Hartley Transform (HT) which seems to fulfill these requirement.

The Fourier analysis is used to convert a picture into an equivalent form which can be more easily processed. In the case of the orthogonal transforms Fourier transform is one of the transforms, with the following properties :

1. It must be reversible
2. It must be unique : one-to-one mapping
3. The two domains should be orthogonal

$$W(t; f) = e^{-j2\pi ft} = \cos(2\pi ft) - j\sin(2\pi ft)$$

To observe the similarity and the property of data (correlation) :

$$\int_{-\infty}^{\infty} s(t)\sin(2\pi ft)\,dt = S_R(f) \text{ :REALpart of Fourier Transform}$$

$$\int_{-\infty}^{\infty} s(t)\cos(2\pi ft)\,dt = S_I(f) \text{ : IMAGINARY part of Fourier Transform}$$

The complex Fourier spectrum is defined as:

$$S(f) = S_R(f) - j\,S_I(f)$$

The picture data are represented in two parts with the FFT approach :

1. Magnitude: M(f) = $\sqrt{S_R^2(f) + S_I^2(f)}$
2. Phase: $f(f) = arc\tan\frac{S_I(f)}{S_R(f)}$

The major problem of Fourier Transform is a computational limitation resulting from the phase spectrum (Phase Wrapping) : linearity that progresses to infinity. To resolve this computational problem related to the phase spectrum of Fourier transform, two types of solutions may be used :

1. The first solution consists of an algorithmic approximation to the phase,
2. The second solution consists to extend the Fourier transform with a best solving of its phase problem. Therefore, Hartley Transform was proposed.

The Hartley Transform requires new transform operations to extend the Fourier approach :

$$W_H(t, f) = \cos(2\pi ft) + \sin(2\pi ft)$$

$$S_H(f) = S_R(f) + S_I(f) = M(f)(\cos\phi(f)+\sin\phi(f))$$

$$S_R(f) = M(f)\cos\phi(f)$$

$$S_I(f) = M(f)\sin\phi(f)$$

The advantage of the Hartley Transform results from the function that contains information about the phase without a computational complexity. The picture data are represented by the Hartley Transform as follows:

3. Magnitude: $M(f) = \sqrt{S_R^2(f) + S_I^2(f)}$
4. Phase: $V(f) = \dfrac{S_H(f)}{M(f)} = \cos\phi(f)+\sin\phi(f))$

5.1.4.4.2.Procedure

To study the use of the Hartley Transform, we have performed the following experiments:

1- Use the HT of the images of the same chip without defect.
2- We have calculated the phase of the images
3- Use the HT of the images of the same chip with defect.
4- We have calculated the spectral phase of the images
5- We have performed the following comparisons:
  - Spectral phase of the chip1_image 1 and chip1_image 2
  - Spectral phase chip1_image 1 and chip1_image 5
  - Spectral phase of the average of chip1_images 1, 2, 3 and 4 with the chip1_image 1
  - Spectral phase of the chip1_image 1 and def1_image 1
  - Spectral phase chip1_images 1,2,3 and 4 and def1_image 1

- Spectral phase of the average of chip1_images 1, 2, 3 and 4 with the def1_image 1,2,3 and 4

5.1.4.4.3.Results

The following table contains the results of the comparison between good and defected chips using the Hartley transform.

	Mean Difference	Mean of A	Mean of B
A=chip1_image1 and B=chip1_image2	0.01	-0.004	-0.001
A=chip1_image1 and B=chip1_image5	0.01	-0.004	-0.006
A=chip1_image1 and B = average chip1_image1,2,3 and 4	0.008	-0.004	0.004

Table 3. Comparison between the HT spectral phase of the different images taken at different instant for PCBs with the same chip with good solder join

From this tables, we notice that the integration over the time has increased the accuracy of the acquisition. This is represented by the decrease of the mean error between the integrated images and the actual images. Comparing this Table 3 to Table 2 , it seems that the FFT phase is less sensitive to the acquisition noise (lighting) than the HT phase. The Application of both transforms on the different PCBs in the following sections, will give more details about the efficiency of the FFT and HT.

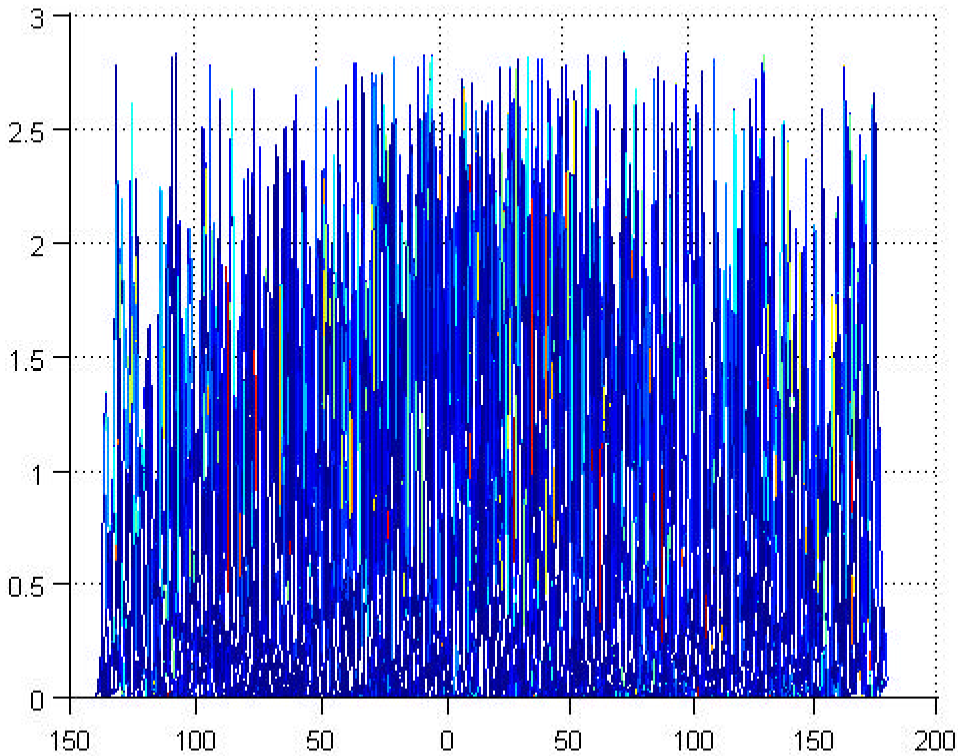

Figure 19. Comparison of the HT phases between chip1_image 1 and def1_image 1 (maximum error = 2.8277 at pixel(8,80), second maximum error =2.824 at pixel(5,102))

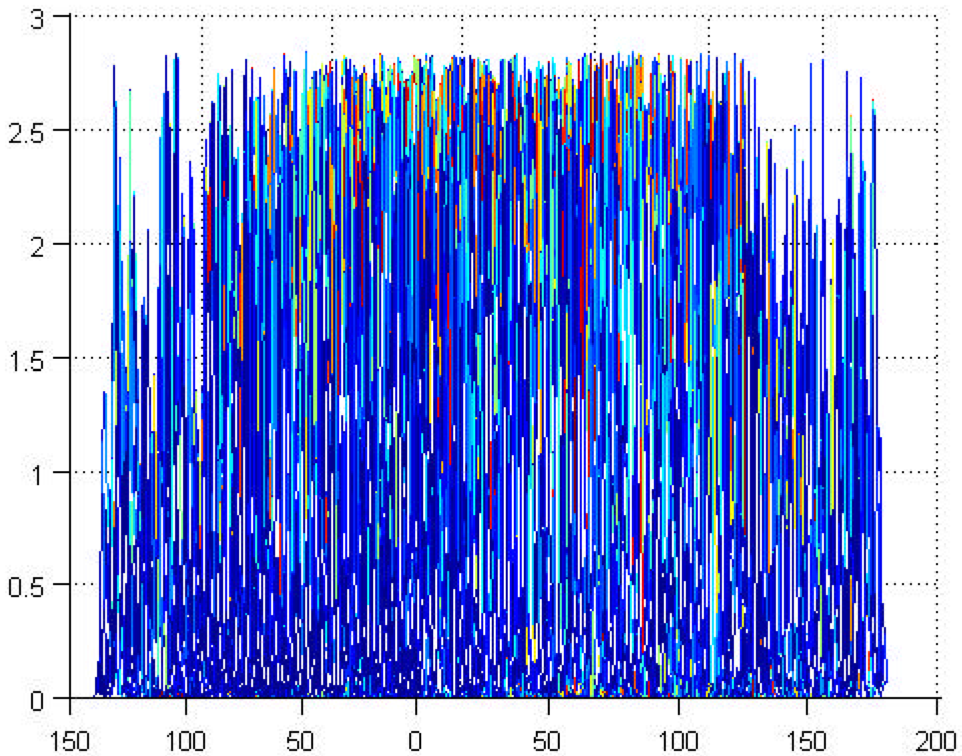

Figure 20. Comparison of the HT phases between the average of chip1_images 1,2,3 and 4 and def1_image 1 (maximum error = 2.828 at pixel(27,106), second maximum error = 2.8278 at pixel(103,49))

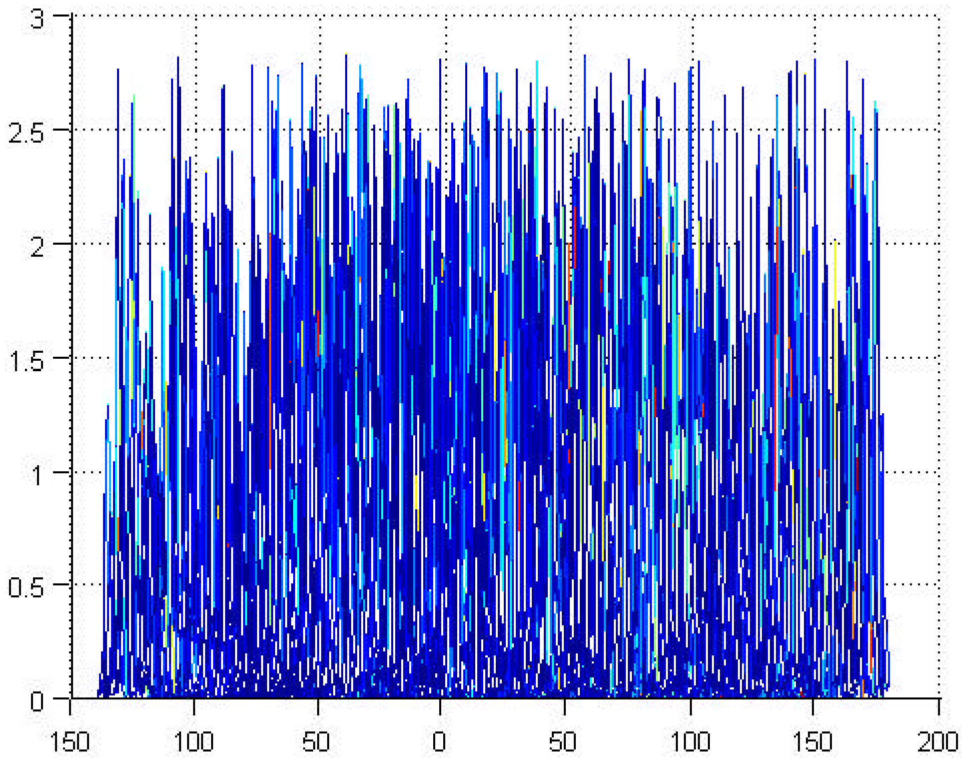

Figure 21. Comparison of the HT phases between the average of chip1_images1,2,3 and 4 and the average of def1_images1,2,3 and 4 (maximum error=2.822 at pixel(79,40), second maximum error=2.809 at pixel(10,67))

From Figure 19, Figure 20, and Figure 21, we notice the following remarks:

- It is quite difficult to locate the relevant information on the HT spectral phase distribution
- The maximum error (about 2.8) is located on several regions depending on the images
- The temporal information (the acquisition noise due to the lighting conditions) seems to not affect the spectral phase.
- It is very difficult to evaluate the effect of the integration over the time of the four images. To evaluate this parameter, see the application of this method on the following sections

5.1.4.4.4.Conclusions and recommendations

It is quite difficult to decide about the good feature extraction method. The best evaluation criterion is the application of the different preprocessing methods (FFT magnitude, FFT phase, HT phase, integration) and evaluate their efficiency.

The following section presents a comparison of all these preprocessing methods as an input to the neural network for the inspection of several chips on one kind of PCB boards.

5.1.5. Application

We have applied the presented concepts on some images using the back-propagation neural network and Elman neural network. To validate these results, several images are needed for different acquisition of the same kind of board. At moment of writing this document 8 images are available in our database, which is not enough to validate the results but sufficient to study the behavior of neural networks using different preprocessing methods. We have chosen to train the neural network on 6 images and to test it on the remaining images. Table 4 and Table 5 contain the obtained results. The following notations have been used:

MSE and gradient: mean square error and gradient from the neural network

FFT Magnitude: the features are taken around the frequency 0 and around the last column and the first row

HT: Hartley transform

Estimation error: it is the mean of the absolute differences between the expected output and the real output

Feature extraction method	MSE	Gradient	Estimation Error
FFT Magnitude (features around frequency zero)	$1.2\ 10^{-13}$	$4.9\ 10^{-11}$	0.053
FFT Magnitude (features around frequency zero and last column first row)	$3.5\ 10^{-15}$	$3.9\ 10^{-11}$	0.056
FFT Phase	10^{-15}	$3\ 10^{-11}$	0.047
HT spectral phase	$6.5\ 10^{-18}$	$9.3\ 10^{-11}$	0.037

Table 4. Experiment results using the different feature extraction methods with the feed-forward back-propagation neural network

Feature extraction method	MSE	Gradient	Estimation Error
FFT Magnitude (features around frequency zero)	$3.3\ 10^{-14}$	$2.8\ 10^{-11}$	0.042
FFT Magnitude (features around frequency zero and last column first raw)	$2.7\ 10^{-14}$	$2.9\ 10^{-11}$	0.042
FFT Phase	$4.5\ 10^{-15}$	$3.4\ 10^{-11}$	0.040
HT spectral phase	$3.2\ 10^{-18}$	$9.8\ 10^{-19}$	0.031

Table 5. Experiment results using the different feature extraction methods with the Elman neural network

From Table 4 and Table 5, we notice that neural network using the HT spectral phase as a feature extraction method has given the best results. This is represented by the small value of the estimation error comparing to the use of the FFT. To validate these results, this algorithms should be applied to several PCBs.

5.2. Rainfall-Runoff project

The aim of the this project is to estimate the actual runoff from a water source to a dam according to a previous runoff and the actual rainfall. This is very important in order to forecast a flood in a dam to better manage and handle the water scattering to the different customers. Therefore, a mathematical and computational model using the neural network should be built to give an accurate estimate according to an available database for 10 years ago. The objective of this project is very clear and very useful for the society of the Mediterranean region with suffer the rarity of the water resources. Thus, it is worth to well handle them in a optimal manner.

This project is under investigation. A previous work has been already performed RD002. The results seems very encouraging. We have tried to implement some different models and compare the results with those of the already implemented models. We have a database from 10 years. Two matrix R1 and R2 of 10x365. R1 represents the daily averaged rainfall measured from different pluviometers. R2 represents the daily runoff from a section. For software reasons the matrices values have been normalized between 0 and 1.

Some experiments has been performed using these database using the Elman and the feed-forward neural network. The first 8 years have been using for the training where the last two years have been used for the tests. Table 6 contains the obtained results.

MSE and gradient: mean square error and gradient from the neural network

Estimation error: it is the mean of the absolute differences between the expected output and the real output

Neural Network	MSE	Gradient	Estimation Error
Feed forward	$6\ 10^{-3}$	$3\ 10^{-4}$	0.055
Elman	$7\ 10^{-4}$	$9.5\ 10^{-8}$	0.042

Table 6. Experiment results using the feed-forward back-propagation and the Elman neural networks for the estimate of the runoff

From these results, we notice that the Elman neural network gives better results than the feed-forward network. To validate this results, more experiments should be performed.